An evaluation of ANN methods for estimating the lengths of hydraulic jumps in U-shaped channel

Larbi Houichi, Noureddine Dechemi, Salim Heddam and Bachir Achour

ABSTRACT

Modelling of hydraulic characteristics of jump using theoretical and empirical models has always been a difficult task. The length of jump may be defined as the distance measured from the toe of the jump to the location of the surface rise. Due to high turbulence this length cannot be determined easily by theory. However, it has been investigated experimentally so as to design the stilling basins with hydraulic jumps. In this work, the control of a hydraulic jump by broad-crested sills in a U-shaped channel is recalled theoretically and experimentally examined. The study begins with a multiple regression (MR) analysis. Then, and in order to model the relative lengths of hydraulic jumps, we have implemented and evaluated two different artificial neural networks (ANN): multilayer perceptron neural network (MLPNN) and generalized regression neural network (GRNN). The results demonstrate the predictive strength of GRNN and its potential to predict hydraulic problems with an adaptive spread value. However, the MLPNN model remains best classified by these indexes of performance.

Key words | artificial neural network, GRNN, lengths of hydraulic jump, MLPNN, MR, U-channel

Larbi Houichi
Research Laboratory in Applied Hydraulics,
Department of hydraulics,
University of Batna,
Algeria

Noureddine Dechemi
Laboratory Construction and Environment,
Polytechnical National School,
Alger,
Algeria

Salim Heddam (corresponding author)
Faculty of Science,
Department of Agronomy,
University of Skikda,
Algeria
E-mail: *heddamsalim@yahoo.fr*

Bachir Achour
Research Laboratory in Subterranean and Surface hydraulics,
University of Biskra,
Algeria

NOMENCLATURE

A Cross-sectional area of flow [m^2]
D Diameter [m]
Fr Froude number [–]
L_j Length of jump [m]
Q Discharge [m^3/s]
g Acceleration due to gravity [m/s^2]
h Depth of flow [m]
q Specific discharge [–]
y Relative depth of flow [–]
θ_1 Angle for semicircular cross-sectional area [rad]

ABBREVIATIONS

ANN Artificial neural networks
GRNN Generalized regression neural network
MLPNN Multilayer perceptron neural network
MR Multiple regression

doi: 10.2166/hydro.2012.138

INTRODUCTION

The hydraulic jump is the discontinuous transition between supercritical and subcritical flow with varied or fixed location (Vischer & Hager 1998), it is characterized by a sudden increasing of the water surface with high turbulence production. This phenomenon is an example of steady non-uniform flow. Principally, the hydraulic jump is well known to hydraulic engineers as a useful means of dissipating excess energy of flowing water downstream of hydraulic structures, such as spillways, chutes and sluices (Hager 1992). Some of the other practical applications are: e.g. flow-metering flume, mixing of chemicals for water purification and aerating water (Chow 1981; Kucukali & Cokgor 2007). In practice, the stilling basin is seldom designed to confine the entire length of a free hydraulic jump on the paved apron, because such a basin would be too expensive. Consequently, accessories to control the jump are usually installed in the basin. The main purpose of such control is to shorten the range within which the jump will take place

and thus to reduce the size and cost of the stilling basin (Chow 1981).

The hydraulic jump in open non-rectangular channels has been studied by many researchers. Mentioning in this context the circular and U-shaped channel; in the circular one, the jump was considered by Hager (1992), Stahl & Hager (1999), Achour (2000), Dey (2001), Gargano & Hager (2002) and Mitchell (2008). Moreover in the U-shaped one, the jump was also considered by Silvester (1964), Rajaratnam (1964), Hager (1989), Houichi (2001), Achour & Debabeche (2003) and Afzal & Bushra (2006). The length of jump may be defined as the distance measured from the toe of the jump to the location of the surface rise (Rajaratnam 1967). This definition was adopted and used within the current study. In theory, the length cannot be determined easily because of the effects of highly turbulent flow. This phenomenon continuously modifies the internal jump characteristics. Yet, it has been investigated experimentally (Chow 1981; Kréménetsky *et al.* 1984). In nature, turbulent flow, rollers and eddies, the random nature of surface disturbances, and air entrainment, complicate the exact determination of the two ends of a hydraulic jump. In practice, the end of a hydraulic jump is considered to be the point from which the concrete coating is not necessary any more (Lencastre 1996).

Neural networks have been successfully applied in a number of diverse fields including hydraulic problems. In their excellent paper, Coulibaly *et al.* (1999) put forward a full state-of-the-art review of research on artificial intelligence (AI), especially concerning artificial neural networks (ANNs); though few attempts have so far been made to analyse the hydraulic jump phenomenon using AI. Recently Raikar *et al.* (2004) introduced the application of ANNs to determine the end-depth-ratio for a smooth inverted semicircular channel in all flow regimes. Omid *et al.* (2005) adopted an ANN approach to model sequent depth and jump length in gradually expanding jumps having rectangular and trapezoidal sections for a wide range of divergent angles and side wall slopes. ANN models were developed by Güven *et al.* (2006) to simulate the mean pressure fluctuations beneath a hydraulic jump occurring on sloping stilling basins. Especially, generalized regression neural network (GRNN) is widely used in different science activities and environment applications, such as in the work of Heddam *et al.* (2011).

The main objective of the present study is the presentation and evaluation of two different ANN techniques: multilayer perceptron neural network (MLPNN) and GRNN, in order to predict the relative length for hydraulic jumps in a U-shaped channel controlled by broad-crested sills.

THEORETICAL ANALYSIS

In a horizontal or weak slope channel, a solution to the hydraulic jump under rapid flow transition circumstances cannot be found using a specific energy diagram. Instead, the momentum equation is used. This approach is perhaps the most popular theoretical approach towards the hydraulic jump. Using the definition sketch shown in Figure 1, a theoretical equation is developed by Houichi (2001) and Achour & Debabeche (2003) for the sequent depth (h_1, h_2) of the hydraulic jump in U-shaped channels as:

$$\frac{32q^2}{\theta_1-\sin\theta_1\cos\theta_1}-(\theta_1-\sin\theta_1\cos\theta_1)\cos\theta_1-\frac{2}{3}\left(1-\sin^3\theta_1\right)=\frac{8q^2}{\left(y_2-\frac{1}{2}+\frac{\pi}{8}\right)}+\left(2y_2-1+\frac{\pi}{2}\right)(2y_2-1) \quad (1)$$

with:

$$y_1=\frac{h_1}{D}<0.5,\ y_2=\frac{h_2}{D}\geq 0.5,\ q=\frac{Q}{\sqrt{gD^5}}$$

and:

$$\theta_1=\cos^{-1}(1-2y_1),\ \mathrm{Fr}_1=\frac{8q\sqrt{\sin\theta_1}}{(\theta_1-\sin\theta_1\cos\theta_1)^{1.5}}$$

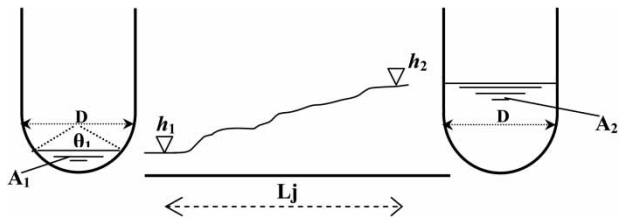

Figure 1 | Definition sketch for hydraulic jump in U-shaped horizontal channel; Area A_1 in semicircular and Area A_2 in U.

In Equation (1), q is specific discharge calculated knowing the discharge Q and the diameter D. θ_1 is the angle at the centre of the circle between the lines connecting it to the water surface at the boundary, calculated knowing the first sequent depth h_1 and the diameter D. y_1 and y_2 are relative sequent depth respectively upstream and downstream of jump. Equation (1) which is implicit for the sequent depth of hydraulic jump, may be solved by a trial and error procedure and can be graphically presented as shown in Figure 2.

EXPERIMENTS AND EXPERIMENTAL RESULTS

Figures 3 and 4 show an overall view of the experimental model. The experiments were performed in a horizontal U-shaped channel, 6 m in length, 0.245 m in diameter and

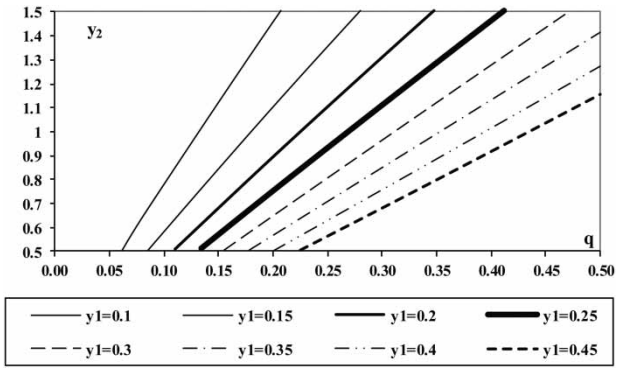

Figure 2 | Theoretical variation of y_2 with q for various values of y_1 according to Equation (1).

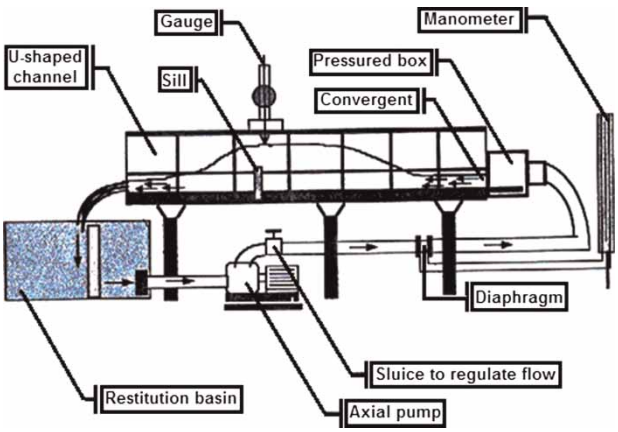

Figure 3 | Schematic view of experimental device.

Figure 4 | Hydraulic jump controlled by a broad sill in U-channel.

0.7 m in total depth. The semicircular bed was made of PVC (polyvinyl chloride): it is surmounted by two vertical side walls of which one is of metal and the other is of transparent plexiglass allowing the visualization of the flow. In each of the experiments, water is supplied through a closed flume by an axial pump. The flows Q, measured by a diaphragm flowmeter, range between 3 and 30 l/s. The incident flow is generated by a convergent box (CB) to provide different initial flow depths and Froude numbers into the channel. The toe of the hydraulic jump was pushed near to the CB so that the opening a_0 becomes similar to the first sequent depth of the jump ($h_1 \approx a_0$). The jumps were controlled by a series of broad sills which were positioned at a known distance. The depths h_2 of the flow were measured using a point gauge with a reading accuracy of $\pm$ 0.5 mm that was placed on rails at the top of the channel. The lengths L_j of jumps were evaluated with a graduated ribbon with a reading accuracy of $\pm$0.1 m. The experimentation related to six series of tests each corresponding to one of six initial depths $h_1 = 1.0$, 1.60, 2.4, 3.4, 5 and 6.1 cm or $y_1 = 0.0408$, 0.0653, 0.0979, 0.13, 0.2041 and 0.2490. Low values of h_1 were voluntarily considered in order to define especially their influence on the relative lengths of jump. Table 1 summarizes the experimental data range. The appendix gives the obtained experimental

Table 1 | Experimental data range

Parameters	Range
First sequence depth (h_1)	1.0–6.1 cm
Second sequence depth (h_2)	12.5–35 cm
Length of jump (L_j)	125–275 cm
Discharge (Q)	3.0–27.4 l/s
Incident Froude Number (Fr_1)	2.46–25.45

measurements (available online at http://www.iwaponline.com/jh/015/138.pdf). All experimental values ($0.04 \leq y_1 \leq 0.25$, $0.51 \leq y_2 \leq 1.43$ and $0.03 \leq q \leq 0.3$) are included in the complete theoretical range ($0 < y_1 < 0.5$, $0.5 < y_2 < 1.5$ and $0 < q < 0.5$).

ARTIFICIAL NEURAL NETWORKS

Multilayer perceptron neural network (MLPNN)

ANNs are analogue computational systems whose structure is inspired by studies of the human brain. ANNs may be defined as structures comprised of densely interconnected adaptive simple processing elements that are capable of performing massively parallel computations for data processing and knowledge representation. Many different architectures of neural network have been developed to tackle a variety of problems. In the current paper we have only investigated one of the most simple and also most popular networks, namely the MLPNN (Rumelhart & McClelland 1986), because it is capable of approximating any function with a finite number of discontinuities (Hornik *et al.* 1989) as long as sufficient training is performed.

The MLPNN is a nonparametric technique for performing a wide variety of detection and estimation tasks (Haykin 1994). As shown in Figure 5, the MLPNN consists of three layers: an input layer, an output layer and one or more hidden layers. Each layer is composed of a predefined number of neurons. The neurons in the input layer only act as buffers for distributing the input signals a_i to neurons in the hidden layer, n is the number of input variables chosen in the input layer. Each neuron j in the hidden layer sums up its input signals a_i after weighting them with the strengths of the respective connections w_{ij} from the input layer, b is the bias term (or threshold) and computes its output value y_j of the neuron as a function f of the sum:

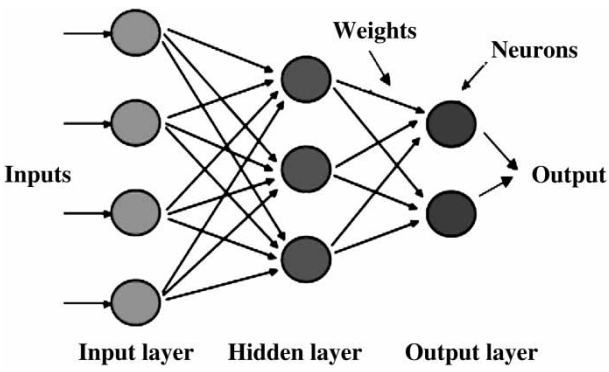

Figure 5 | Schematic diagram of MLPNN.

$$y_j = \mathrm{f}\left(\sum_{\mathrm{i}}^{n} w_{ij}\, a_i + b\right) \tag{2}$$

The output of neurons in the output layer is similarly computed. The mean squared error (*MSE*) between the desired and actual values of the output neurons E is defined as:

$$E = \frac{1}{2}\sum_{j}^{N}\left(y_{\mathrm{d}j} - y_i\right)^2 \tag{3}$$

where N is the number of data used, $y_{\mathrm{d}j}$ is the desired value of output neuron j and y_j is the actual output of that neuron. Each weight w_{ji} is adjusted to reduce E as rapidly as possible. The adjustment w_{ji} depends on the adopted training algorithm (Haykin 1994).

Generalized regression neural network (GRNN)

The GRNN is a neural network architecture that can solve any function approximation problems in the sense of estimating a probability distribution function. The network was first developed by Specht (1991). It approximates any arbitrary function between input and output vectors, drawing the function estimate directly from the training data. We can also note that GRNNs perform regression where the target variable is continuous. The GRNN will consider a few non-linear aspects of the estimated problem.

As shown in Figure 6, the GRNN consists of four layers, including the input layer, pattern layer, summation layer and output layer. The first layer is fully connected to the second pattern layer where each unit represents a training input pattern and its output is a measure of the distance of the input from the stored patterns. Each pattern layer unit is connected to the two neurons in the summation layer:

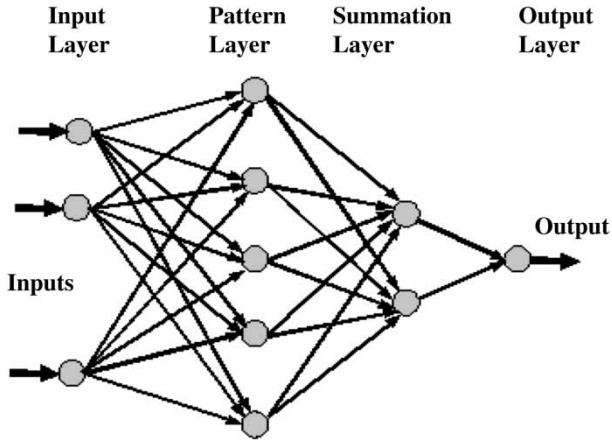

Figure 6 | Schematic diagram of GRNN.

S-summation neuron and *D*′-summation neuron. The *S*-summation neuron computes the sum of the weighted outputs of the pattern layer while the *D*′-summation neuron calculates the unweighted outputs of the pattern neurons. The output layer merely divides the output of each *S*-summation neuron by that of each *D*′-summation neuron, yielding the predicted value Y_i to an unknown input vector x as:

$$Y_i = \frac{\sum_{i=1}^{M} y_i \,.\, \exp[-D'(x\,,\,x_i)]}{\sum_{i=1}^{M} \exp[-D'(x\,,\,x_i)]} \tag{4}$$

where M indicates the number of training patterns and the Gaussian D' function in (4) is defined as:

$$D'(x, x_i) = \sum_{k=1}^{m} \left(\frac{x_k - x_{ik}}{\sigma}\right)^2 \tag{5}$$

y_i is the weight connection between the ith neuron in the pattern layer and the *S*-summation neuron, m is the number of elements of an input vector, x_k and x_{ik} are the jth element of x and x_i respectively. The σ notation, known as the spread (or width), determines the generalization performance of the GRNN. In general, a larger σ value may result in better generalization: its optimal value is determined via trial and error. It should be noted that in conventional GRNN applications all units in the pattern layer have the same single spread.

ANALYSES OF REGRESSION AND ANN MODELS

Jump lengths estimation approach

Empirical methods are basically regression models developed from fitting curves to measured experimental data. Figure 7 shows the scatterplot matrix created as a matrix of two variable scatterplots for all pairs of variables. All parameters should be undertaken as inputs (q, y_1, Fr_1 and y_2) to explain the relative lengths of hydraulic jumps L_j/h_2 or L_j/h_1. The choice is mainly based on Equation (1) which indicates how parameters are connected and also based on literature (Silvester 1964; Rajaratnam 1967; Hager 1992). Excluding any variable induces unimproved results.

An approach equation can be obtained by multiple regression (MR) analysis using the backward elimination method for relative lengths of hydraulic jump L_j/h_2 and L_j/h_1 knowing values of q, y_1, Fr_1 and y_2.

$$\frac{L_j}{h_2} = 23.27 + 85.51q - 59.34y_1 + 0.37\mathrm{Fr}_1 - 24.71y_2 \tag{6}$$

$$\frac{L_j}{h_1} = 113.8 + 967.21q - 485.03y_1 + 12.35\mathrm{Fr}_1 - 266.29y_2 \tag{7}$$

Equations (6) and (7) consider simultaneously the upstream influence of y_1 and q.

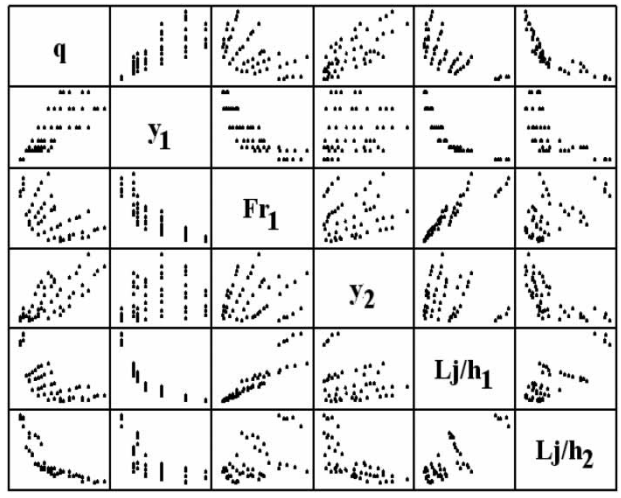

Figure 7 | Matrix plot for all data and all pairs of variables.

The experimental relative lengths L_j/h_{2exp}, L_j/h_{1exp} of jumps are compared in Figures 8 and 9 with their counterparts L_j/h_{2pred}, L_j/h_{1pred} obtained by approach relations (6) and (7). The root *MSE*s for these models are equal to *RMSE* = 0.87, 15.30 and the coefficients of determination equal to $R^2 = 0.930$, 0.950 respectively.

Let us remember that *RMSE* describes the average difference between experimental data and model predictions, while coefficient of determination R^2 is a measure of how much of the original uncertainty in the data is explained by the model.

Multilayer perceptron neural network models

Two alternatives have been considered to have two different outputs. The output is the relative length value of hydraulic jump L_j/h_2 or L_j/h_1. The inputs are (q, y_1, Fr_1 and y_2) as undertaken in the regression section.

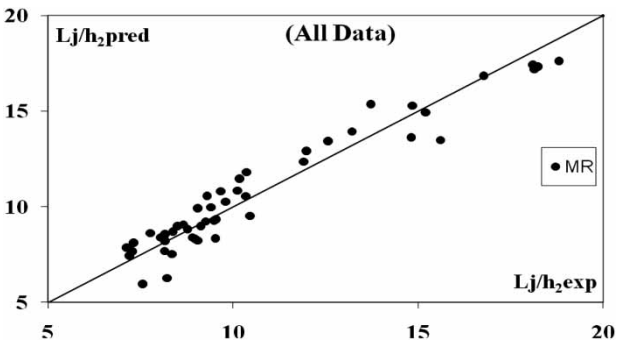

Figure 8 | Predicted versus experimental L_j/h_2 values for the MR model according to Equation (6).

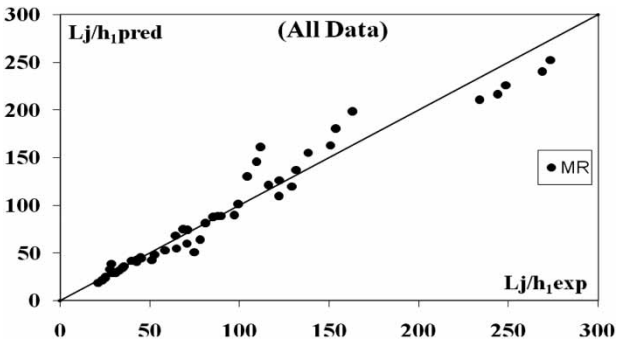

Figure 9 | Predicted versus experimental L_j/h_1 values for the MR model according to Equation (7).

A difficult task with the MLPNN method is choosing the number of hidden nodes. Yet, there is no theory to tell how many hidden units are needed to approximate any given function. The optimal determination of number of neurons in the hidden layer is the issue of a trial (results of Matlab) which has been verified by altering the iteration number to achieve the best performance values (*RMSE* and R^2). The activation function used is the *tansig* function.

Generalized regression neural network models

With the same considerations about inputs-outputs, (q, y_1, Fr_1 and y_2) and separately outputs (L_j/h_2 or L_j/h_1), the robust model in this type of ANN is required to apply a spread which will yield the most suitable performance with an adaptive value and it proves useless to change this in the present study.

Results of both models and different outputs

The best network structure is respectively given in Table 2 and Table 3 for the L_j/h_2 and L_j/h_1 outputs. As seen from Table 2, the best model for predicting the relative length values of hydraulic jumps L_j/h_2 is MLPNN with the lowest *RMSE* (0.41843) and highest R^2 (0.99202) value for the validation phase, so GRNNs have a remarkably similar performance.

The models consist of four inputs and seven neurons in the hidden layer for the MLPNN and the spread value equal to 0.3 for the GRNN. For both models, the graphical representation is respectively given in Figures 10 and 11 for training and validation phases.

As seen from Table 3, the best model for predicting the relative length values of hydraulic jumps L_j/h_1 is also MLPNN which is characterized by the lowest *RMSE* (4.90587) and highest R^2 (0.99496) value for the validation phase. It consists of 4 inputs and 3 neurons in the hidden layer. The GRNN model with the same spread value equal to 0.3 is also competing. The graphical representation is given in Figures 12 and 13 for training and validation phases for both models. Continually, in the present study, both ANN models are better than the MR model.

Table 2 | The performance values of MLPNN and GRNN models for L_j/h_2 output

	GRNN		MLPNN		MR
Performance index	**Training**	**Validation**	**Training**	**Validation**	**All data**
R^2	0.99068	0.96304	0.99896	0.99202	0.92927
RMSE	0.30483	0.69109	0.10143	0.41843	0.87161

Table 3 | The performance values of MLPNN and GRNN models for L_j/h_1 output

	GRNN		MLPNN		MR
Performance index	**Training**	**Validation**	**Training**	**Validation**	**All data**
R^2	0.99857	0.98885	0.99567	0.99496	0.94715
RMSE	2.49140	7.37180	4.32344	4.90587	15.29641

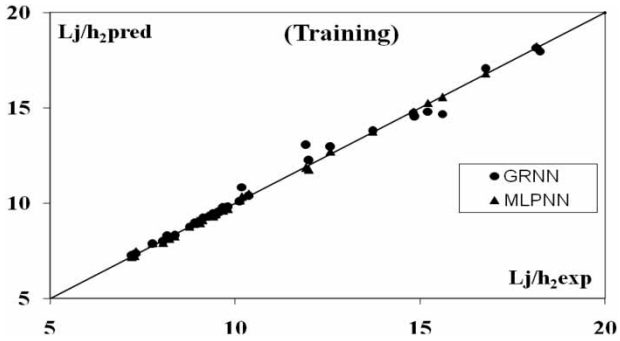

Figure 10 | Predicted versus experimental L_j/h_2 values for the GRNN and MLPNN models for training phase.

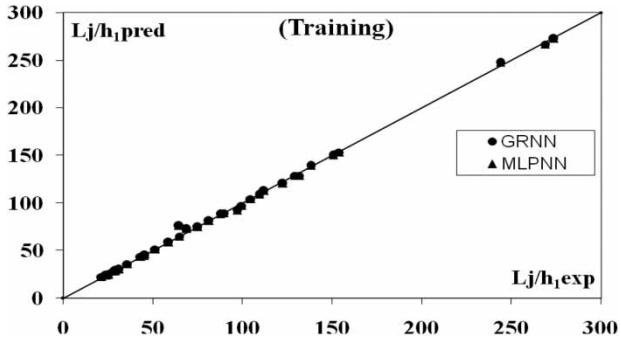

Figure 12 | Predicted versus experimental L_j/h_1 values for the GRPNN and MLPNN models for training phase.

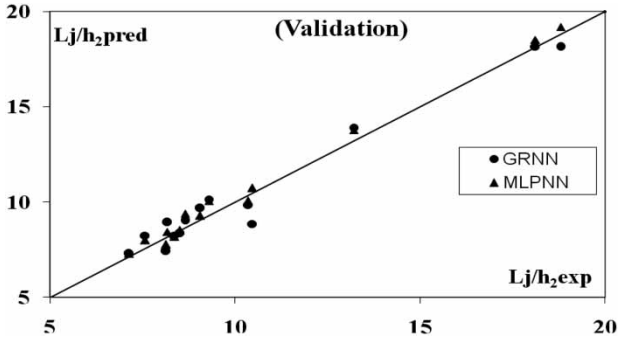

Figure 11 | Predicted versus experimental L_j/h_2 values for the GRNN and MLPNN models for validation phase.

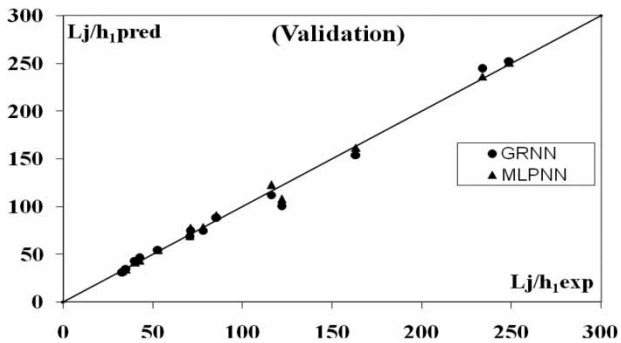

Figure 13 | Predicted versus experimental L_j/h_1 values for the GRPNN and MLPNN models for validation phase.

By examining the tables of values and the graphs corresponding, particularly in the validation phase, the results also show that modelling the lengths of hydraulic jumps as L_j/h_1 is more robust than the usual form L_j/h_2. Moreover this statement is confirmed for the MR model ($R^2 = 0.92927$ for L_j/h_2 and $R^2 = 0.94715$ for L_j/h_1).

CONCLUSIONS

Modelling the relative lengths of hydraulic jumps for convenient conceptions of hydraulic structures is very useful when it is not easy to determine these lengths theoretically. In this work we have used MR and ANN techniques to predict the relative lengths L_j/h_2 and L_j/h_1. The comparison of these various models, considering all independent variables (q, y_1, y_2, Fr_1), shows that both MLPNN and GRNN give comparable results for the training and the validation. The best model for predicting is given by applying MLPNN technique with the *tansig* function of activation. At the same time, GRNNs persist as a competitive process by using an adaptive spread value equal to 0.3. Besides, the study shows that both ANN models outperform the MR technique. By examining the tables of values and the corresponding graphs, particularly in the validation phase, the results also show that modelling the lengths of hydraulic jumps as L_j/h_1 is more robust than the usual form L_j/h_2. This remark is also confirmed for the MR model.

In future, two possible extensions of our work can be suggested: including other AI techniques to the same channel studied here, as well as extending the techniques already used to study hydraulic jumps in the case of prismatic and non-prismatic rough and sloped channels.

REFERENCES

Achour, B. 2000 Hydraulic jump in a suddenly widened circular channel. *J. Hydraul. Res.* **38** (4), 307–311.

Achour, B. & Debabeche, M. 2003 Ressaut contrôlé par seuil dans un canal profilé en U (Control of hydraulic jump by sill in a U-shaped channel). *J. Hydraul. Res.* **41** (1), 97–103.

Afzal, N. & Bushra, A. 2006 Hydraulic jump in circular and u-shaped channels. *J. Hydraul. Res.* **44** (4), 567–576.

Chow, V. T. 1981 *Open-Channel Hydraulics*, 17th edition, International Student Edition. McGraw-Hill, Tokyo.

Coulibaly, P., Anctil, F. & Bobée, B. 1999 Prévision hydrologique par réseaux de neurones artificiels: état de l'art (Hydrological forecasting using artificial neural networks: the state of the art). *Can. J. Civ. Eng.* **26**, 293–304.

Dey, S. 2001 Hydraulic jump in circular and semicircular channels. *Dam Eng.* **11** (4), 261–272.

Gargano, R. & Hager, W. H. 2002 Undular hydraulic jump in circular conduits. *J. Hydraul. Eng.* **12** (11), 1008–1013.

Güven, A., Günal, M. & Çevik, A. 2006 Prediction of pressure fluctuations on sloping stilling basins. *Can. J. Civ. Eng.* **33** (11), 1379–1388.

Hager, W. H. 1989 Hydraulic jump in u-shaped channel. *J. Hydraul. Eng.* **115** (5), 667–675.

Hager, W. H. 1992 *Energy Dissipators and Hydraulic Jump*. Kluwer Academic Publishers, Dordrecht.

Haykin, S. 1994 *Neural Networks: A Comprehensive Foundation*, 1st edition. Prentice Hall, Upper Saddle River, NJ.

Heddam, S., Bermad, A. & Dechemi, N. 2011 Applications of radial basis function and generalized regression neural networks for modelling of coagulant dosage in a drinking water treatment: a comparative study. *ASCE J. Environ. Eng.* **137** (12), 1209–1214.

Hornik, K., Stinchcombe, M. & White, H. 1989 Multilayer feedforward networks are universal approximators. *Neural Netw.* **2**, 359–366.

Houichi, L. 2001 Etude d'un dissipateur d'énergie à profil géométrique en U (Study of an Energy Dissipator with U-geometrical Profile). Master's Thesis in Hydraulic Works. University of Batna, Algeria.

Kréménetsky, N., Schtérenliht, D., Alychev, V. & Yakovléva, A. 1984 *Hydraulique*. Mir Editions, Moscow.

Kucukali, S. & Cokgor, S. 2007 Fuzzy logic model to predict hydraulic jump aeration efficiency. *Proc. Inst. Civ. Eng., Water Manage.* **160** (4), 225–232.

Lencastre, A. 1996 *Hydraulique Générale*. Editions Eyrolles, Paris.

Mitchell, S. 2008 Hydraulic jump in trapezoidal and circular channels. *Proc. Inst. Civ. Eng., Water Manage.* **161** (3), 161–167.

Omid, M. H., Omid, M. & Esmaeeli, V. M. 2005 Modelling hydraulic jumps with artificial neural networks. *Proc. Inst. Civ. Eng., Water Manage.* **158** (2), 65–70.

Rajaratnam, N. 1964 Discussion to Silvester. Hydraulic jump in all shapes of horizontal conduits. *J. Hydraul. Div. ASCE* **90** (HY4), 341–350.

Rajaratnam, N. 1967 Hydraulic jumps. *Adv. Hydrosci. Acad. Press* **4**, 197–280.

Raikar, R. V., Kumar, D. N. & Dey, S. 2004 End depth computation in inverted semicircular channels using ANNs. *Flow Meas. Instrum.* **15**, 285–293.

Rumelhart, D. E. & McClelland, J. L. 1986 *Parallel Distribution Processing: Exploration in the Microstructure of Cognition*. MIT Press1, Cambridge, MA.

Silvester, R. 1964 Hydraulic jump in all shapes of horizontal channel. *J. Hydraul. Div. ASCE* **90** (HY1), 23–55.

Specht, D. F. 1991 A general regression neural network. *IEEE Trans. Neural Netw.* **2** (6), 568–576.

Stahl, H. & Hager, W. H. 1999 Hydraulic jump in circular pipes. *Can. J. Civ. Eng.* **26** (3), 368–373.

Vischer, D. L. & Hager, W. H. 1998 *Dam Hydraulics*. John Wiley and Sons Ltd, Zürich.

First received 17 October 2011; accepted in revised form 14 June 2012. Available online 21 September 2012